Smart Structures and Systems, *Vol. 30, No. 3 (2022) 263-271*
https://doi.org/10.12989/sss.2022.30.3.263

On the development of data-based damage diagnosis algorithms for structural health monitoring

Anne S. Kiremidjian*

Department of Civil and Environmental Engineering, Stanford University, 478 Via Ortega, Stanford, CA 94022, USA

(*Received June 12, 2022, Revised July 17, 2022, Accepted July 17, 2022*)

Abstract. In this paper we present an overview of damage diagnosis algorithms that have been developed over the past two decades using vibration signals obtained from structures. Then, the paper focuses primarily on algorithms that can be used following an extreme event such as a large earthquake to identify structural damage for responding in a timely manner. The algorithms presented in the paper use measurements obtained from accelerometers and gyroscope to identify the occurrence of damage and classify the damage. Example algorithms are presented include those based on autoregressive moving average (ARMA), wavelet energies from wavelet transform and rotation models. The algorithms are illustrated through application of data from test structures such as the ASCE Benchmark structure and laboratory tests of scaled bridge columns and steel frames. The paper concludes by identifying needs for research and development in order for such algorithms to become viable in practice.

Keywords: auto-regressive models; damage algorithms; damage classification; damage detection; vibration data; wavelet transform models

1. Introduction

A civil structure, whether it be a building, a bridge, or a crane, has many similarities to the human body with the skeleton resembling its framing and the body's lifelines representing the utilities. In the past three decades there has been significant advances in the state of the art in structural health monitoring (SHM) technology in many ways mimicking that of the human health diagnostic systems. Many of the developments have also been empowered with the use of machine learning and data science techniques. An SHM system can be thought of consisting of two major components: (1) Sensors and sensor communications network; and (2) Decision support system. The decision support system (Kiremidjian *et al*. 2009) includes the damage diagnosis algorithms and the health prognosis algorithms. A critical component of the decision support system is the availability of information communication module. Fig. 1 shows schematically the components of a SHM system.

Most frequently, the sensors deployed on structures are accelerometers. In recent years, cameras, global positioning systems (GPS), tilt meters, humidity, temperature, gyroscope and fiber-optic strain sensors have been deployed to obtain more accurate measurements of the state of the structure. There are ongoing efforts to develop damage specific sensors, such as material dependent crack detection sensors (e.g., Chakraborty *et al*. 2019, Roach 2009, Albishi and Ramahi 2017). However, there is still a significant need for developing sensor for specific types of damage. With advances of micro-electromechanical (MEMS) sensors and increased microprocessor capacity, complex sophisticated sensing systems have been introduced (e.g., Straser 1998, Lynch *et al*. 2004, Kiremidjian *et al*. 2009, Snowfort 2017). Such sensing systems include the sensor (e.g., MEMS accelerometer, temperature, humidity and strain), the microprocessor which serves the purpose of controlling the device, collect data and possibly analyze the data locally, and a communication component. The ability to analyze data on the sensing unit microprocessor represents a major advantage over systems that require complete data packets to be transmitted in order to be analyzed at a remote location.

The sensing units are interconnected through a sensor communications network. Such networks can be hardwired physical systems or wireless communications networks. Issues with connectivity, transmission distance and fidelity of wireless communications systems are continuously being overcome, making such systems viable. For wired systems, installation of wires in existing buildings and other structures remains to be a main challenge in terms of labor and costs.

Sensor location, density and distribution is increasingly a nonissue as the cost of sensors or complex sensing units is continuously decreasing. Significant work has been done to determine the optimal number of sensors and their locations (e.g., Guo *et al*. 2004, Cantero-Chinchilla *et al*. 2020) but using more than an optimal number does not represent a major obstacle and in some cases may be beneficial as they

*Corresponding author, Ph.D., Professor,
E-mail: ask@stanford.edu
The C. L. Peck, Class of 1906 Professor in the School of Engineering, Stanford University, Stanford CA 94305

ISSN: 1738-1584 (Print), 1738-1991 (Online)

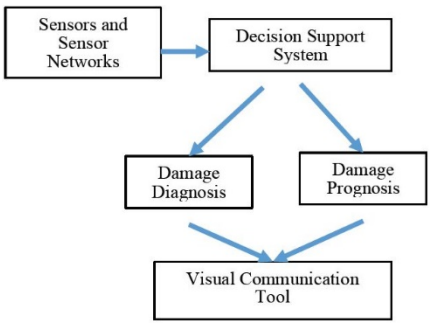

Fig. 1 Components of a structural health monitoring system (SHM)

provide redundancy and stability.

While the hardware technology is advancing very fast and is providing viable solutions, the main challenge that persists is having a decision support system that informs the user. The decision support system typically consists of several key components. The first of these is the data diagnostic tool(s). The diagnostic tool uses the data collected from the structure and attempts to (1) identify the occurrence of damage, (2) localize the damage and (3) quantify the damage. Quantification of the damage involves identifying the type of damage and its severity. It is not sufficient, for example to be able to say that we have identified a crack at a steel beam-to-column joint. We need to be able to predict the crack length and width to classify the crack into a specific pre-defined category.

Two main approaches have been considered for damage diagnosis. These include system identification and statistical pattern recognition, machine learning and general data science methods. Key difference in the two approaches is that system identification methods require data from the entire system to be collected synchronously, downloaded to a main computing environment, and perform computationally very expensive analyses to identify damage. In the data driven approaches, the damage identification is typically based on individual sensor measurements or perhaps a small group of measurements. Localization of damage is limited typically to a few damage incidences or general area of where the damage might be, requiring further inspection of the structure. Quantification of damage has been somewhat successful for large amounts of damage but remains a challenge for small amounts of damage – for example, yielding of an I-beam that is taking place only part way in the flange is very difficult to identify while formation of a complete hinge on a member can be identified. Similarly, large displacements of a structure can be detected relatively easily but small one not so much. It should also be pointed out that gradually occurring damage is particularly difficult to identify and quantify. Damage to extreme loads, such as those due to earthquakes or strong wind can more easily be diagnosed provided the damage is sufficiently large.

The second component of the decision support system is the structural life prognosis, which attempts to determine what is the residual strength and life of the structural components or system. Research in this area has been very limited and continues to be a major challenge. Ideally, we would like to be able to tell if the structure has sufficient integrity to continue to be used and for how long it can be used. The decisions and predictions of useful strength and life, however, depend heavily on the ability to provide robust diagnosis. Thus, until our diagnostic tools get to a point where we can reliably identify, localize and quantify the damage, we will not be able to provide the prognostic component of the overall health monitoring problem.

While these observations may seem ominous, they should not prevent us from attempting to build systems that capture the structural health monitoring diagnostic and prognostic components. What needs to be done is to recognize the limitations, quantify the uncertainty with any diagnostic and prognostic prediction and provide alternative approaches for actions to remedy the problem. Consequences from each action will need to be specified for more rational decision making.

An integral component of the decision support system is the information delivery module. This module can visually and factually provide the results from the diagnostics and prognostics in a format that is understandable to decision makers. As mentioned previously, the step after the diagnostics and prognostics will have to be the follow-on actions each with defined consequences and likelihood of these consequences to occur. For example, a damage diagnosis that specifies hinge formations at key locations on a column can lead to a localized failure or a catastrophic failure of the structure. Each outcome should be informed with additional analysis that also includes uncertainty estimations. The two possible outcomes require that decisions be made to repair the structure or replace the structure each with corresponding direct costs and indirect costs resulting from each outcome. Providing the decision makers with likelihoods for each outcome – decision pair (for this example – localized damage or catastrophic failure with follow on actions of repair or replacement of the structure), can lead to more rational and defensible decision.

In this paper we summarize several data-based algorithms that can be used for either long term health or extreme event monitoring. Our intention is not to provide a comprehensive coverage of the large volume of research conducted on this topic, but to highlight some of the methods used for identifying damage and correlating it to pre-defined damage states. Most of the algorithms are simple. They were developed with the objective that they can be embedded on a microchip to enable almost instantaneous analysis and information delivery. The details of the algorithms presented in this paper are available in previously published literature. Thus, only the highlights of these algorithms are summarized.

The paper concludes with discussion on the needs for further research, algorithm verification through additional testing and field experimentation, and the development of software for the overall decision support system.

2. Damage detection algorithms

The algorithms summarized in this paper include the autoregressive (AR) model with hypothesis testing and with Gaussian Mixture damage diagnosis, the wavelet-based

algorithms with wavelet energies as damage sensitive features, and the rotation algorithm that uses accelerometer and gyroscope measurements. The three types of algorithms represent a sample of models developed by the author and her students. In each case, a summary of each formulation is first presented, and sample results are then shown. The advantages and potential applications of each algorithm are discussed in each section.

The damage detection algorithms presented in this paper use the measurements from a single or multiple sensors. Thus, for all algorithms the first step is to filter the noise and detrend the signal. For some of the algorithms, the signal is also standardized (or normalized) in order to remove environmental and variable load conditions. For numerically simulated data, the filtering component can be omitted, but for laboratory or field data, filtering is a key part performed prior to any analysis. Not all algorithms require standardization. With each algorithm we will identify if this step is needed. When needed, a signal $\{x(t), 0 < t < t_n\}$ is standardized (or normalized) by subtracting its mean m_{ij} and normalizing it to its standard deviation, s_{ij}, resulting in the signal $\{x^*(t), 0 < t < t_n\}$.

The damage detection is typically performed at individual sensor locations. Signals from undamaged states are collected first and then signals are collected during and/or after an event. Damage diagnosis needs to be done following the occurrence of extreme or unusual loading. However, deterioration due to normal loading conditions is also very important to detect and, in such cases, signals need to be collected periodically and tested for significant changes in the signature of the signal. Thus, the diagnostic component requires a comparison of two signals and identifying a significant change in the characteristics of the signals. If signals are collected during an extreme event, alternative approach may be used where the change in the signature of the extreme event signal is detected.

Initially, when the structure is known to be in an undamaged state, signals need to be collected under different temperature, humidity, and time of day conditions. The measurements are influenced by these conditions; therefore, a library of such signals needs to be gathered. When comparing subsequent signals that are obtained from potentially damaged structure to signals from an undamaged structure, the signal from the undamaged structure needs to come from similar temperature, humidity, and time of day conditions as those of the potentially damaged structure. Three types of algorithms are summarized in the next subsections.

2.1 AR algorithms with statistical hypothesis testing and Gaussian mixture model classification

In this approach low amplitude accelerations are collected either periodically or before and after an extreme event. An Autoregressive Moving Average (ARMA) model is fitted through the data from undamaged and potentially damaged structures. The signals are always standardized before fitting the ARMA model and the order of the ARMA model is first ascertained using the Akaike information criterion (AIC) (see Nair *et al*. 2006). The signals are divided into streams of equal length. The general form of the ARMA model for the j^{th} stream of signal i, $\{x_{ij},(t)\}$, is

$$x_{ij}(t) = \sum_{k=1}^{p} \alpha_k x_{ij}(t-k) + \sum_{k=1}^{q} \beta_k \varepsilon_{ij}(t-k) + \varepsilon_{ij}(t) \quad (1)$$

Where a_k and b_k are the AR and MA coefficients, respectively, and p and q are the corresponding orders.

The damage sensitive feature, *DSF*, is defined by Eq. (2)

$$DSF = \frac{\alpha_1}{\sqrt{\alpha_1^2 + \alpha_2^2 + \alpha_3^2}} \quad (2)$$

Where a_1, a_2, and a_3 are the first three AR coefficients. Comparison of the *DSFs* in Eq. (2) from the damaged and undamaged structures are shown to capture the occurrence of damage. Statistical significance testing is performed to further affirm that the values of the *DSFs* from the two streams are significantly different implying that damage has occurred in the structure.

The algorithm was tested with several experimental data including the ASCE Benchmark Structure (Johnson *et al*. 2000) and a test of a four bay, three piers and two abutments one-quarter scale bridge subjected to gradually increasing earthquake ground motion performed at the University of Nevada, Reno.

Fig. 2 shows the results from the application of the model to the ASCE Benchmark Structure. The structure is a four-story steel braced frame with 16 unidirectional

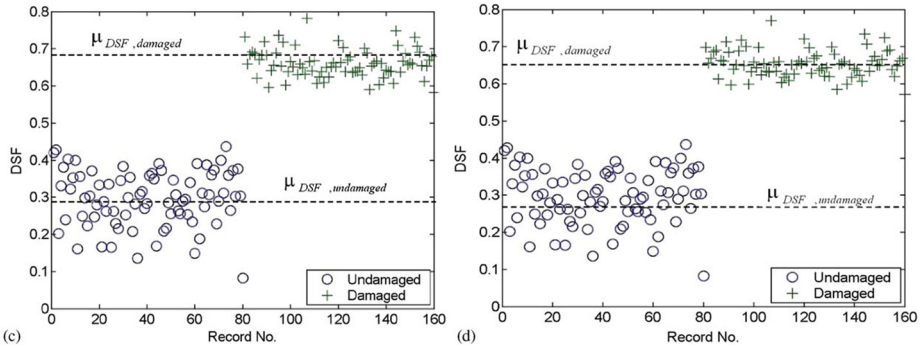

Fig. 2 Separation of *DSF* clouds from damaged and undamaged structures for damage patterns 3 (a) and 4 (b) (Modified from Nair *et al*. 2006)

accelerometers at various locations. Six damage patterns are defined with damage states one through four corresponding to various braces being removed. Damage state 5 is the same as damage state four plus bolt loosening and damage state six represents a reduction in the stiffness of a single brace. In Fig. 2 the clouds of *DSFs* from the undamaged and damage patterns 3 and 4 are shown, as well as the mean values of each cloud.

From Fig. 2, it can be observed that the clouds are clearly separated. Statistically significant testing further confirms that the *DSF* is able to capture the change that has occurred in the structure. It should be noted that the results were not as conclusive when the amount of damage is small such as loosening of a bolt. Most importantly, Nair *et al*. (2006) also showed analytically that the derivatives of the alpha coefficients with respect to the stiffness are directly proportional to one over the square root of the stiffness, thus implying that even small change in the stiffness will be manifested in the alpha coefficients, making the *DSF* particularly desirable.

A second algorithm that uses the alpha coefficients of the AR component of the ARMA model was first proposed by Nair and Kiremidjian in 2007. In this algorithm the *DSFs* are the first three AR coefficients without any functional form as was done in the previous algorithm. The fundamental premise in this model is that the damage sensitive features represented by the first three AR coefficient can be separated into different classes coming from the different signals. The Gaussian Mixture Model (GMM) is used as the clustering algorithms to identify different classes of feature clusters. A GMM with M classes (or mixtures) has the following form

$$f(X_{1:N}) = \sum_{i=1}^{M} \pi_i \phi_i(X; \theta_i) \tag{3}$$

where, $\boldsymbol{X}$ is the collection of **N** feature vectors, $f_1 \sim N(m_i, s_i)$ is a Gaussian vector with mean vector $\boldsymbol{m}_i$ and covariance matrix $\boldsymbol{S}_i$, and p_i is the non-negative mixture weight for each class. The unknown parameters of the GMM Q = $\{m_i, \boldsymbol{S}_i, p_i: i = 1, 2, \ldots, M\}$ are estimated using maximum likelihood principles (see Nair and Kiremidjian 2007 for further details).

Damage is identified if more than one mixture is in the dataset based on the premise that the AR coefficients from a damaged and undamaged states of the structure will form distinct clouds identified by the GMM model. Classification of clusters is achieved by determining the number of clouds in the mixture. For this purpose, the gap statistic is used to determine the optimal number of clusters and the distance between features is used to define a measure of dispersion.

The extent of damage is then estimated using the Mahalanobis distance. This metric is often used to establish the separation between multivariate distributions. Eq. (4) defines the Mahalanobis distance between two vectors $\boldsymbol{y}$ and z with a covariance matrix $\boldsymbol{S}$.

$$\Delta(y, z; \Sigma) = \sqrt{(y - z)^T \Sigma^{-1} (y - z)} \tag{4}$$

The damage extent can, then, be defined as

$$DM = \frac{\Delta(\mu_{undamaged}, \mu_{damaged}, \Sigma_{undamaged})}{\Delta(\mu_{undamaged}, 0, \Sigma_{undamaged})} \tag{5}$$

Where $\boldsymbol{m}$ is the mean of each cluster and $\boldsymbol{S}$ is its covariance matrix between two clusters. Eq. (5) defines the damage measure in terms of the Mahalanobis distance presented in Eq. (4)

The model is illustrated through an application to the ASCE Benchmark Structure (Johnson *et al*. 2000) described earlier in the paper. The gap statistics was used to determine the number of clusters and in this case correctly predicted six classes of clusters. The Gaussian mixture model parameters were then obtained for the collection of clusters. The Gaussian mixture model was effective in identifying the different damage patterns. Although Fig. 3 shows the results for the case of major damage, minor and moderate damage states not shown here were also discriminated successfully (see Nair and Kiremidjian 2007). All six damage patterns showed significant separation.

The Mahalanobis distance, ***DM***, for each damage pattern was also obtained and is shown in Fig. 4. From the figure it can be observed that the damage measure ***DM*** captures the degree of damage very effectively for all six damage patterns, although there is little difference between damage pattern four and five as expected. The damage in pattern five identical to the damage pattern four with the bolt loosening added. Again, the classification is not able to distinguish this small change in the structural damage occurrence.

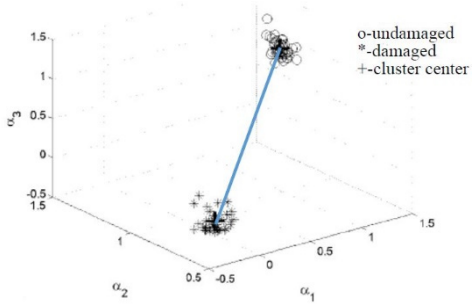

Fig. 3 Example separation of undamaged cluster and damage pattern 2 corresponding to brace removal on the first and third floors of the structure (Modified from Nair and Kiremidjian 2007)

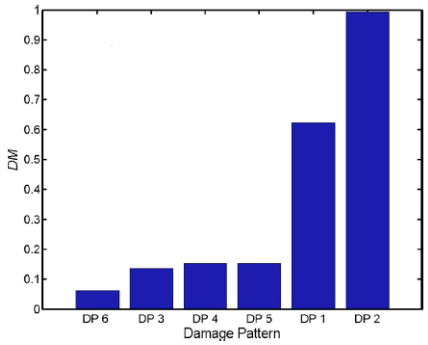

Fig. 4 Variation of the Mahalanobis distance ***DM*** for each damage pattern of the Benchmark Structure (Modified from Nair and Kiremidjian 2007)

2.2 Wavelet-based algorithms

In this section we discuss algorithms that use the wavelet transform to define a damage sensitive feature. The continuous wavelet transform of a function $f(t)$ is given by

$$Wf(a,b) = \int_{-\infty}^{+\infty} f(t)\frac{1}{\sqrt{a}}\psi^*\left(\frac{t-b}{a}\right)dt \quad (6)$$

Where ψ^* is the complex conjugate of the mother wavelet scaled by a and translated by b.

Two types of algorithms were developed using the wavelet transform. The first uses ambient (low amplitude) vibration signals before and after damage has occurred, and the second uses the signal from an extreme event (large amplitude vibrations) to identify damage. For the low amplitude signals the Haar wavelet is used to obtain the wavelet energies. The Haar wavelet is defined as follows

$$\psi(t) = \begin{bmatrix} 1 & \text{for} & 0 \le t < 0.5 \\ -1 & \text{for} & 0.5 \le t < 1.0 \end{bmatrix} \quad (7)$$

The wavelet coefficients of a vibration signal are obtained from the following equation

$$W_H f(a,b) = \frac{j}{2\pi\sqrt{a}}\int_{-\infty}^{+\infty}\frac{F(s)}{s}\exp(jsb)\left[1-exp\left(\frac{jas}{2}\right)\right]^2 \quad (8)$$

Where F(s) is the Fourier transform of the signal and $j=\sqrt{-1}$. Nair and Kiremidjian (2009) showed that the wavelet coefficients of a vibration signal are related to the stiffness of the structure thus they can be used as indicators of damage. Similar conclusions are obtained also with the Morlet wavelet (Nair and Kiremidjian 2009).

The algorithm was again applied to the low amplitude data obtained from the ASCE Benchmark Structure. The *DSF* is defined as the energy of the wavelet coefficients at the sixth dyadic scale of the Haar wavelet denoted as E_6. Several different scales were tested before selecting the sixth scale. In general, the specific scale to be used for damage detection will need to be ascertained for each structure prior to application of the algorithm. Damage is considered to occur when the mean of the *DSF* (m_{DSF}) migrates with each new vibration measurement. Fig. 5 shows an example of the migration of the mean of the DSF for damage pattern 3 of the test structure. The differences between the mean values are further tested and are found to be statistically significantly different.

From the figure it can be observed that the data are scattered but the mean values are well separated. Similar results are also obtained with the application of the Morlet wavelet.

The second wavelet-based algorithm presented here uses strong motion vibration signals to ascertain that damage has occurred. The main advantage of using the wavelet transform is that it captures that time-varying characteristics of a vibration signal as is typically the case with earthquake motion. The algorithm was developed primarily for structural vibrations caused by earthquake ground motion.

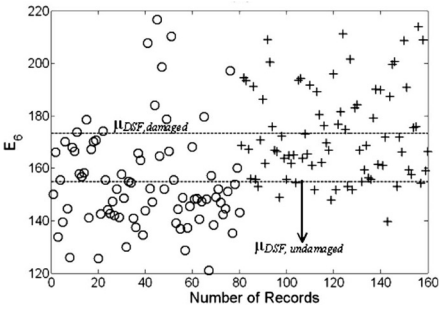

Fig. 5 Migration of the wavelet based mean *DSF* for damage pattern 3 of the ASCE Benchmark Structure (Modified from Nair and Kiremidjian 2009)

For this purpose, it is found that the Morlet wavelet best captures the variations of the signal. It has the best Heisenber box, (Mallat 1999, Hong and Kim 2004).

The Morlet wavelet is given as

$$\psi(t) = e^{jw_0 t}e^{\frac{t^2}{2}} \quad (9)$$

Where w_0 is the center of the Fourier transform of the mother wavelet. Determining the center frequency requires additional analysis (see Noh *et al*. 2011). For simplicity only the real part of the Morlet wavelet is used and the wavelet energy at a particular scale a, $E_{scale(a)}$, is defined as follows

$$E_{scale(a)} = \sum_{b=1}^{K} |Wf(a, b\times\Delta t_s)|^2 \quad (10)$$

Where K is the number of data points in the time history, Dt_s is the sampling period, and |*| is the absolute value. Noh *et al*. (2011) showed that the wavelet energy at a particular scale captures changes in stiffness, mass and damping of the structure, thus reflecting the occurrence of damage in the structure. More specifically, $E_{scale(a)}$ decreases at scales close to the natural frequency of the first mode of the undamaged structure. The damage sensitive feature using $E_{scale(a)}$ is then defined as follows

$$DSF = 1 - \frac{E_{scale(\hat{a})}}{\sum_{i=M}^{N} E_{scale(a^i)}} \quad (11)$$

Where M and N are the minimum and maximum dyadic scales of the strong motion recording $f(t)$. The *DSF* defined by Eq. (11) varies between zero, when there is no damage, and 1, when the structure has undergone severe damage. This *DSF* is further correlated to story drift ration (*SDR*) to represent different damage states. Fragility functions can then be developed in terms of the *DSF* that can them be used to determine the most likely damage state of the structure.

The sensitivity of the *DSF* defined by Eq. (11) was first verified using 381 simulated strong motions. The simulations were obtained for a four-story steel frame structure. A scaled model of the structure was also tested at the State University of New York, Buffalo (Lignos *et al*. 2011) and the test results were used to verify the numerical

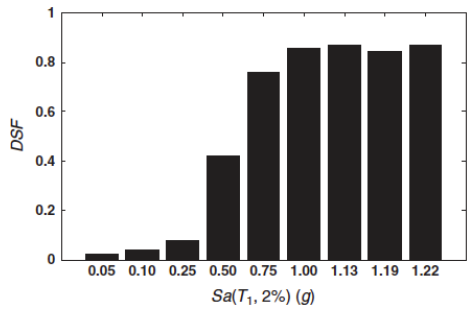

Fig. 6 Variation of the Escale(a) DSF with increasing spectral acceleration for the four-story steel moment frame structure (Modified from Noh *et al*. 2011)

model of the structure used in the simulations. The analytical model of the four-story steel moment resisting frame was also used to simulate different damage levels in the structure. The ground motion from the Andrews hospital from the 1989 Loma Prieta, California earthquake was increasingly scaled to obtain the response motions of the structure. Fig. 6 shows the variation of the DSF with increasing damage to the test structure the ground motions was increased.

Fragility functions were also obtained using the simulated responses of the model structure. Noh *et al*. (2012) showed that the correlation between damage and the proposed *DSF* is higher than that of using story drift ratio (*SDR*) making this *DSF* particularly desirable for damage classification for earthquakes.

2.3 Rotation algorithms

The algorithms presented in Sections 2.1 and 2.2 were shown to be effective and have many advantages over system identification approaches for damage assessment. In particular, the occurrence of damage can be detected from vibration measurements at individual locations. Moreover, the analysis can potentially be performed on a microprocessor at the sensing unit itself provided such computational capabilities are included in the design of the sensing unit. The AR algorithms can be particularly power efficient in ascertaining damage as their computation is relatively simple. The algorithms that use the wavelet energy are considerably more complex thus potentially having higher power requirements.

An algorithm that uses single measurements and can be correlated to story deformation was proposed by Cheung and Kiremidjian (2014). In this particular algorithm, low amplitude vibrations obtained before and after a structure is subjected to strong ground motion are used. If such measurements are not available, the leading and trailing portion of the strong earthquake motion can be used as an alternative. Vibrations in the vertical and one of the horizontal components of motion are required for this purpose. It was observed by the authors that the base line of the vertical and horizontal vibrations after an earthquake that has caused significant deformation to the structure will not be respectively at -1 g and 0 g. This is because after the structure has deformed the orientation of the strong motion

(a) (b)

Fig. 7 Original (a) and rotated (b) position of accelerometer after drift of structure (Modified from Cheung and Kiremidjian 2014)

accelerometer will not be aligned with the original vertical and horizontal direction but will be at an angle q. Fig. 7 shows the orientation of the sensor relative to its original axis before and after the structure has deformed.

The angle q of the new orientation of the instrument is obtained by simple trigonometry as follows

$$\theta = arctan\left(\frac{A'_x}{A'_y}\right) \tag{12}$$

Where A'_x and A'_y are the mean values of the measurements in the x- and y-directions after the structure has deformed. For slender structures or tall columns, the angle can be used to obtain the order of magnitude of the residual displacement of the structure. Estimating the residual displacement of a structure is particularly useful as such displacements can be directly correlated to various damage states.

For bridge columns, for example, the residual displacement can be estimated by taking the length of the column above the plastic hinge at the base of the column. For that purpose, Pauly and Priestley's formula for plastic hinge formation can be used to determine the length above the plastic hinge. The residual displacement at the top of a column, Δ_p, can be obtained from the following equation

$$\Delta_p = \theta_p\left(l - 0.5l_p\right) \tag{13}$$

Where l is the length of the column, l_p is the length of the plastic hinge at the base of the column, and θ_p is the rotation of the column above the plastic hinge.

This algorithm was tested with data from several laboratory test including a test conducted at the University of Nevada, Reno (UNR) and one at the University of California, Berkeley (UCB). Both tests were for a single column subjected to a gradually increasing earthquake ground motion. In both tests, low amplitude white noise vibrations were also collected between strong motion tests. The white noise vibrations were used to obtain the orientation of the sensor after each strong motion. Fig. 8(a) shows the migration of the sensor orientation with each strong motion particularly when the deformation increased as obtained from the test at UNR. Fig. 8(b) shows the direct displacement measurements for the column with each strong motion.

Residual displacements of the test column were obtained assuming zero plastic hinge length and an estimated plastic hinge length from the test itself. Fig. 9 shows a comparison

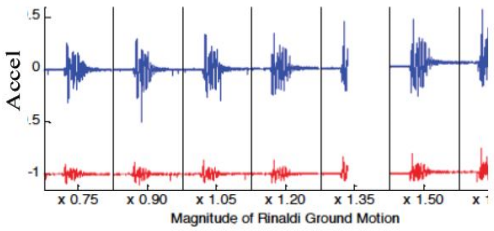

(a)

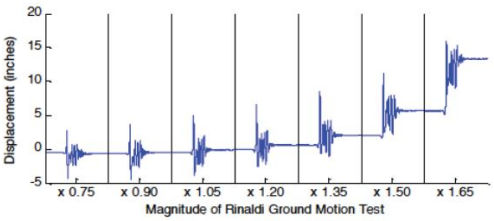

(b)

Fig. 8 Horizontal (blue) and vertical (red) acceleration measurements with increasing ground motion (a) and direct displacement measurements with each ground motion (b) (Modified from Cheung and Kiremidjian 2014)

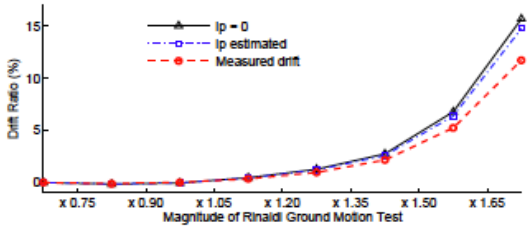

Fig. 9 Comparison of direct displacement measurements to residual displacements estimated from the rotation algorithm (Modified from Cheung and Kiremidjian 2014)

of the displacement measurements to the estimates of residual displacements obtained with the two plastic hinge lengths. From the figure it can be seen that the algorithm overestimates the residual displacement by a large amount if the plastic hinge length is assumed to be zero, but when the proper hinge length is considered, the estimates come very close to the observed displacements. Similar results were obtained with even a better agreement with the test data from the University of California, Berkeley (UBC).

An extension of this algorithm involves multiple sensors distributed along the height of a column or a tall structure. The slope at each sensor location is estimated and a polynomial is fitted through the values of the slopes as functions of the height. By integrating the polynomial function of the slope, an estimate of the deflected shape is obtained. (See Balafas and Kiremidjian 2015a, b). Excellent agreement is obtained between numerically simulated curvatures of test structures and the estimates from measurements. It is shown that the optimal number of sensors needed is four and a fourth order polynomial is sufficient to achieve high accuracy (0.4%) in predicting the curvature of the deformed shape.

A second extension of the rotation algorithm considers measurements from a gyroscope taken in tandem with the accelerometers. A test was designed and conducted at the National Center for Research in Earthquake Engineering (NCREE) at the Taiwan National University. Three-dimensional accelerometers and gyroscopes were installed on two identical scaled three-story structures. In addition, LVDT's were used to measure the direct displacements at each story. One of the structures was damaged by reducing the stiffness of one column (i.e., reducing its cross section).

The objective of this algorithm is to estimate the maximum dynamic displacement that the structure has undergone during the strong motion, thus providing additional information on the potential damage. It is well known that direct double integration of the acceleration signal results in significant error and therefore most frequently in an underestimation of the maximum dynamic displacement. By introducing the complimentary filter, the slope at any instant of time of the signal and subsequently the displacement at that instant is computed obtaining the time history of the displacement of the structure.

For the complimentary filter we first define the angular velocity of the gyroscope at time n as $w(n)$. (See Liao *et al.* 2017 for further detail.) Then the dynamic rotation at time n is

$$\theta(n) = \theta(n-1) + \omega(n)\Delta t \tag{14}$$

To reduce the drift in the gyroscope and the error in the accelerometer measurements, the complementary filter is defined as

$$\theta(n) = \alpha(\theta(n-1) + \omega(n)\Delta t) + (1-\alpha)\theta_a(n) \tag{15}$$

Where $\theta_a(n)$ is obtained from the acceleration measurement at time n and defined by Eq. (14), and a is a filter parameter that varies between 0 and 1 and controls the contribution of the acceleration estimated rotation and the gyroscope estimated rotation.

The algorithm was applied to the data obtained from the three-story structure tested at NCREE. Fig. 10 shows the estimates of the slope as a function of time obtained from the first floor of the damaged structure subjected to one of

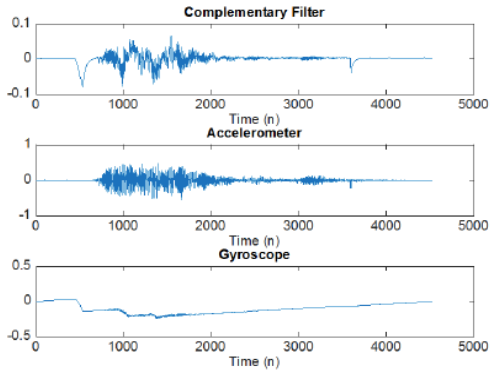

Fig. 10 Estimates of the slope at the first floor of the damaged structure subjected to a Chi Chi Taiwan earthquake ground motion (Modified from Liao *et al.* 2017)

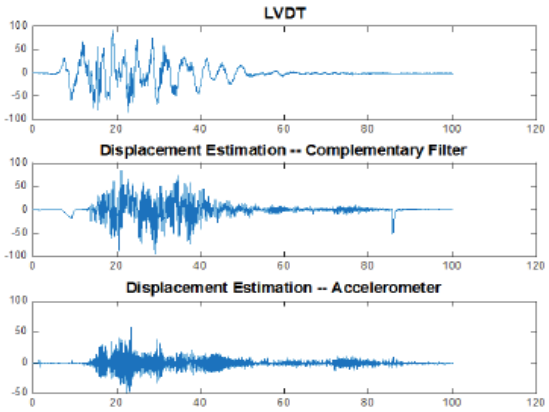

Fig. 11 Displacements (in mm) at the first floor of the damaged structure obtained by the LVDT, from the complementary filter and through direct double integration of the acceleration measurement (Modified from Liao *et al*. 2017)

Table 1 Comparison of estimated and measured peak displacements at story 1 of the damaged structure tested at NCREE (Modified from Liao *et al*. 2017)

Run	LVDT (mm)	Complimentary filter	Accelerometer
1	14.86	20.81	22.44
2	41.79	45.03	47.82
3	59.53	60.92	62.95
4	79.94	81.15	85.08
5	92.44	93.89	114.89
6	117.33	116.60	163.79
7	126.44	128.44	145.67

the ground motions from the 1999 Chi Chi, Taiwan earthquake. Fig. 11 shows the displacement measurements obtained with the LVDT and those estimated using the complimentary filter and those obtained by double integration of the acceleration measurement. Several different a parameters were used, and it was found that best results were obtained with $a = 0.8$.

As it can be seen from Fig. 11, the complimentary filter estimates the maximum dynamic displacement more closely than the double integration. While there is significant noise in the signal from the complimentary filter, it is important to note that we are primarily interested in the maximum dynamic displacement. As can also be seen in Table 1, the maxima from the complimentary filter come very close to the observed values from the LVDT measurements in contrast to the maximum displacement estimates from the double integration of the acceleration signal.

The advantage of using rotation algorithm is that it is easy to apply and can be readily embedded on a microprocessor. Moreover, by estimating both the residual and maximum dynamic displacements, the reliability of the damage forecast increases significantly. Both displacement estimates can be related to potential damage states of a structures following the recommendations of FEMA P-58 (2018) which provides performance limits for the residual and the maximum dynamic displacements.

3. Conclusions

One of the key components of a comprehensive structural health monitoring system is the ability to interpret the data and provide useful information. For that purpose, it is important to have robust and reliable damage diagnosis algorithms. Three different types of algorithms are discussed in the paper. The first set of algorithms use low amplitude ambient vibrations that are obtained before and after damage has occurred on the structure. After filtering and standardizing the signal, either an autoregressive moving average (ARMA) or wavelet model is fit through the vibration signal. For each model it is shown analytically that either the AR coefficients or the wavelet coefficients are sensitive to changes in the stiffness, mass and damping of the structure making them particularly suitable as features for damage detection.

The second class of algorithms use the actual vibration measurements obtained during strong response motion of the structure. The damage sensitive feature, in this case is defined in terms of the wavelet energy computed from the square of the wavelet coefficients. It was shown that this *DSF* is particularly suitable for developing fragility functions for a structure that can be obtained prior to any event and be used as a predictor of the most likely damage state. An advantage of this *DSF* is that it does not require a pre- and post-event low-amplitude motion to be measured. The algorithm was tested with 381 strong response motions obtained from a numerical model that was also laboratory tested and verified. The *DSF* was shown to better correlate to damage than traditionally used story drift ratio (*SDR*).

The third set of algorithms use ambient or low noise measurements before and after an extreme motion to determine the residual and maximum dynamic displacements of the structure. In the absence of low amplitude motions before and after an earthquake, the leading and trailing tails of the strong motion can be used for this purpose. The residual displacement is obtained from the acceleration measurements and the maximum dynamic displacement is estimated by combining the strong motion measurements from the accelerometer and a synchronous gyroscope through a complimentary filter. Very good estimates are obtained with both algorithms. The advantage of this algorithm is that it is simple and can easily be embedded on a computational microprocessor for near-real time damage estimation of a structure subjected to a large event and can provide early warning particularly if there is impending collapse. The residual and maximum dynamic displacements can be directly related to *SDR* limits set for performance levels of structures (FEMA P-58 2018).

While with each algorithm, example applications were illustrated, a significant amount of additional testing is required to determine the efficacy of each DSF and its limitations. The main problem is that systematic data needed for such verifications are still limited particularly for real structures subjected extreme events. All the algorithms presented here share in their simplicity and ability for near real time damage estimation.

Comprehensive damage diagnosis also requires localization and quantification of the damage. Estimating the damage state of the structure is a first step in predicting the amount of damage. FEMA P-58 provides broad range of possible damage classifications for each damage state. For decision support purposes, however, considerably more detailed information is needed. In addition, the algorithms need to be tested under different field conditions to provide reliability and confidence in their predictions. Thus, more research is necessary that focuses on localizing and classifying the damage and significant amount of data need to be generated to test each algorithm.

Acknowledgments

The research described in this paper was financially supported by the Natural Science Foundation, the John A Blume Earthquake Engineering Center, and the John Blume and James Gere Fellowships at Stanford University. The author gratefully acknowledges the contribution of the doctoral students involved in the research – Krishnan Nair, Pooya Sarabandi, Alan Cheung, Hae-Young Noh, Konstantinos Balafas, and Yezheng Liao. In addition, the help of colleagues who enabled us to participate in various laboratory tests or provided key data for testing the algorithms is greatly appreciated. They include Professor Emeritus Seiid Seiidi of the University of Nevada, Reno, the late Professor Steve Mahin of the University of California, Berkeley, and Professor Emeritus H.C. Loh of the National Taiwan University.

References

Albishi, A. and Ramahi, O. (2017), "Microwaves-based high sensitivity sensors for crack detection in metallic materials", *IEEE Transact. Microw. Theory Techniq.*, **65**(5), 1864-1872. https://doi.org/10.1109/TMTT.2017.2673823

Balafas, K. and Kiremidjian, A. (2015a), "Development and validation of a novel earthquake damage estimation scheme based on the continuous wavelet transform of input and output acceleration measurements", *Earthq. Eng. Struct. Dyn.*, **44**(4), 501-522. https://doi.org/10.1002/eqe.2529

Balafas, K. and Kiremidjian, A. (2015b), "Reliability assessment of the rotation algorithm for earthquake damage estimation", *Struct. Infrastr. Eng.*, **11**(1), 51-62. https://doi.org/10.1080/15732479.2013.879318

Cantero-Chinchilla, S., Beck, J., Chiachio, J., Chiachio, M., Chronopoulos, D. and Jones, A. (2020), "Optimal sensor and actuator placement for structural health monitoring via an efficient convex cost-benefit optimization", *Mech. Syst. Signal Process.*, **144**, 106901. https://doi.org/10.1016/j.ymssp.2020.106901

Chakraborty, J., Katunin, A., Klikowicz, P. and Salamak, P. (2019), "Early crack detection of reinforced concrete structure using embedded sensors", *Sensors*, **19**(18), 3879. https://doi.org/10.3390/s19183879

Cheung, A. and Kiremidjian, A. (2014), "Development of a rotation algorithm for earthquake damage diagnosis", *Earthq. Spectra*, **30**(4), 1381-1401. https://doi.org/10.1193/012212EQS016M

FEMA P-58 (2018), "Seismic performance assessment of buildings methodology", Applied Technology Council; Redwood City, CA, USA. https://www.atcouncil.org/docman/fema/246-fema-p-58-1-seismic-performance-assessment-of-buildings-volume-1-methodology-second-edition/file

Guo, H., Zhang, L., Zhang, L. and Zhou, J. (2004), "Optimal placement of sensors for structural health monitoring using improved genetic algorithms", *Smart Mater. Struct.*, **13**(3), 528-534. https://doi.org/10.1088/0964-1726/13/3/011

Hong, J.C. and Kim, Y.Y. (2004), "The determination of the optimal Gabor wavelet shape for the best time-frequency localization using the entropy concept", *Experim. Mech.*, **44**, 387-395. https://doi.org/10.1007/BF02428092

Johnson, E.A., Lam, H.F., Katafygiotis, L.S. and Beck, J.L. (2000), "A benchmark problem for structural health monitoring and damage detection", *Proceedings of 14th Engineering Mechanics Conference*, Austin, TX, USA, May. https://doi.org/10.1142/9789812811707_0028

Kiremidjian, A.S., Sarabandi, P. and Kiremidjian, G. (2009), "A wireless structural monitoring system with embedded damage algorithms and decision support system", *Struct. Infrastr. Eng.*, **7**(12), 881-894. https://doi.org/10.1080/15732470903208773

Lignos, D., Krawinkler, H. and Whittaker, A. (2011), "Prediction and validation of sidesway collapse of two scale models of a 4-story steel moment frame", *Earthq. Eng. Struct. Dyn.*, **40**(7), 807-825. https://doi.org/10.1002/eqe.1061

Lynch, J.P., Sundararajan, A., Law, K.H., Kiremidjian, A.S. and Carryer, E. (2004), "Embedding damage detection algorithms in a wireless sensing unit for attainment of operational power efficiency", *Smart Mater. Struct.*, **13**(4), 800-810. https://doi.org/10.1088/0964-1726/13/4/018

Liao, Y., Balafas, K., Kiremidjian, A., Rajagopal, R. and Loh, C. (2017), "Rapid damage detection from strong motion acceleration and rotation response measurements", *Proceedings of the 16th World Conference on Earthquake Engineering*, Santiago de Chile, Chile, January.

Mallat, S. (1999), *A Wavelet Tour of Signal Processing*, Academic Press, San Diego, CA, USA.

Nair, K.K. and Kiremidjian, A.S. (2007), "Time series based structural damage detection algorithm using Gaussian mixtures modeling", *J. Dyn. Syst. Measure. Control*, **129**(3), 285-293. https://doi.org/10.1115/1.2718241

Nair, K.K. and Kiremidjian, A.S. (2009), "Derivation of a damage sensitive feature using the Haar wavelet transform", *J. Appl. Mech.*, **76**(6), 061015. https://doi.org/10.1115/1.3130821

Nair, K.K., Kiremidjian, A.S. and Law, K.H. (2006), "Time series-based damage detection and localization algorithm with application to the ASCE benchmark structure", *J. Sound Vib.*, **291**(2), 349-368. https://doi.org/10.1016/j.jsv.2005.06.016

Noh, H.Y., Nair, K.K., Lignos, D.G. and Kiremidjian, A.S. (2011), "On the use of wavelet based damage sensitive features for structural damage diagnosis using strong motion data", *J. Struct. Eng.*, **137**(10), 1215-1228. https://doi.org/10.1061/(ASCE)ST.1943-541X.0000385

Noh, H., Lignos, D., Nair, K. and Kiremidjian, A. (2012), "Development of fragility functions as a damage classification/ prediction method for steel moment-resisting frames using a wavelet-based damage sensitive feature", *Int. J. Earthq. Eng. Struct. Dyn.*, **41**(4), 681-696. https://doi.org/10.1002/eqe.1151

Roach, D. (2009), "Real time crack detection using mountable comparative vacuum monitoring sensors", *Smart Struct. Syst., Int. J.*, **5**(4), 317-328. https://doi.org/10.12989/sss.2009.5.4.317

Snowfort (2017), Sensor Network: Open & Wireless for Data Analytics. https://web.stanford.edu/group/snowfort/

Straser, E.G. (1998), "A modular, wireless damage monitoring system for structures", Report No. 128; John A Blume Earthquake Engineering Center, Department of Civil and Environmental Engineering, Stanford University: Stanford, CA, USA.